Supplement of

Disrupted Flow Memory and Synchrony in the Mekong River under Dam Regulation and Climate Change: Implications for Tonle Sap Reverse Flow

Khosro Morovati et al.

Correspondence to: Fuqiang Tian (tianfq@mail.tsinghua.edu.cn)

This supplementary file includes three sections (S1–S3), six figures (Figures S1–S6), and two tables (Tables S1 and S2).

S1. Bathymetry

The approach employed to generate regional bathymetry using 250 cross-sections yielded relatively high accuracy. Figure S1 compares a measured river cross-section at the Phnom Penh Port station in 1999 with the corresponding cross-section derived from our method. Despite some local discrepancies, the overall shape of the predicted cross-section closely aligns with the observed profile.

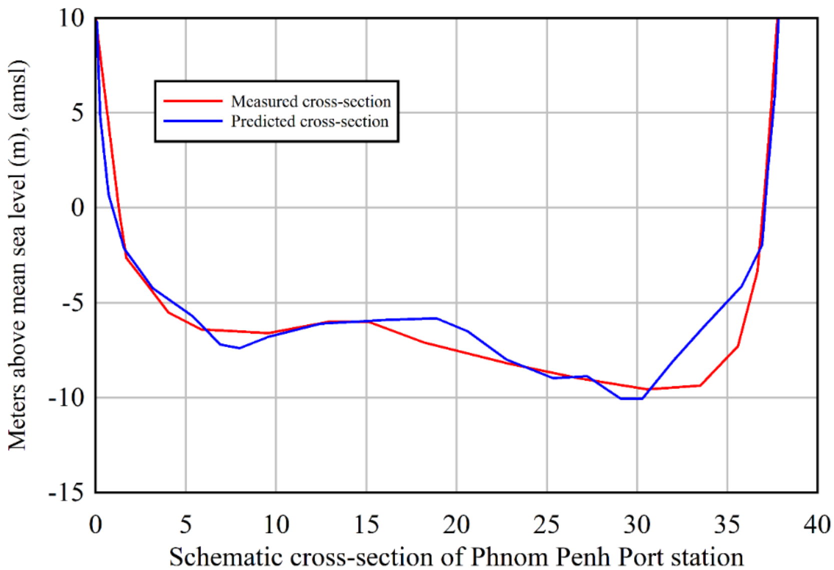

Figure S1. Comparison between the measured river cross-section at Phnom Penh Port station (1999) and the interpolated cross-section generated using the employed bathymetric reconstruction approach. See Figure 1, part (a), for station location.

S2. Additional information for Hydrological Model (THREW)

Figure S2 illustrates the discretization of the entire Mekong River Basin into 651 REWs, enabling spatially explicit representation of diverse hydrological processes across varying climatic and topographic gradients.

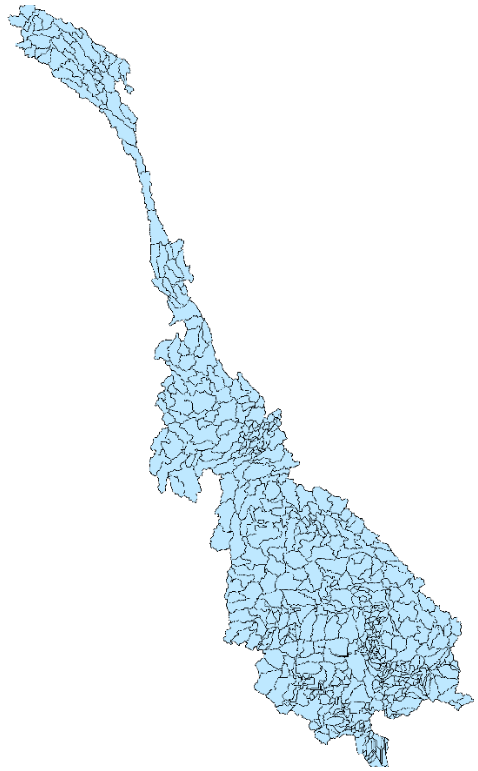

Figure S2. Spatial distribution of 651 REWs covering the Mekong River basin as implemented in the THREW hydrological model.

The model demonstrates several unique attributes that set it apart from conventional hydrological models, attributable to its physically based and spatially distributed framework. Principally, the THREW model utilizes the REW technique for spatial delineation, facilitating the segmentation of the research area into distinct hydrological zones within the REWs. This methodology effectively captures landscape diversity and its associated hydrological reactions, thereby providing a precise portrayal of watershed dynamics. Table S1 gives information on the calibrated parameters in the THREW model and their explanations.

Table S1. Calibrated parameters and their explanation

Parameter	Explanation
kv	Fraction of the potential transpiration rate over the potential evaporation
nt	Roughness of slope
KKA	Exponential coefficient in subsurface runoff calculations
nr	The roughness of the river channel
KKD	The linear coefficient in subsurface runoff calculation
B	Shape coefficient
WM	Average water storage capacity (m)
K	Storage factor in the Muskingum Method
X	Flow ratio factor in the Muskingum Method

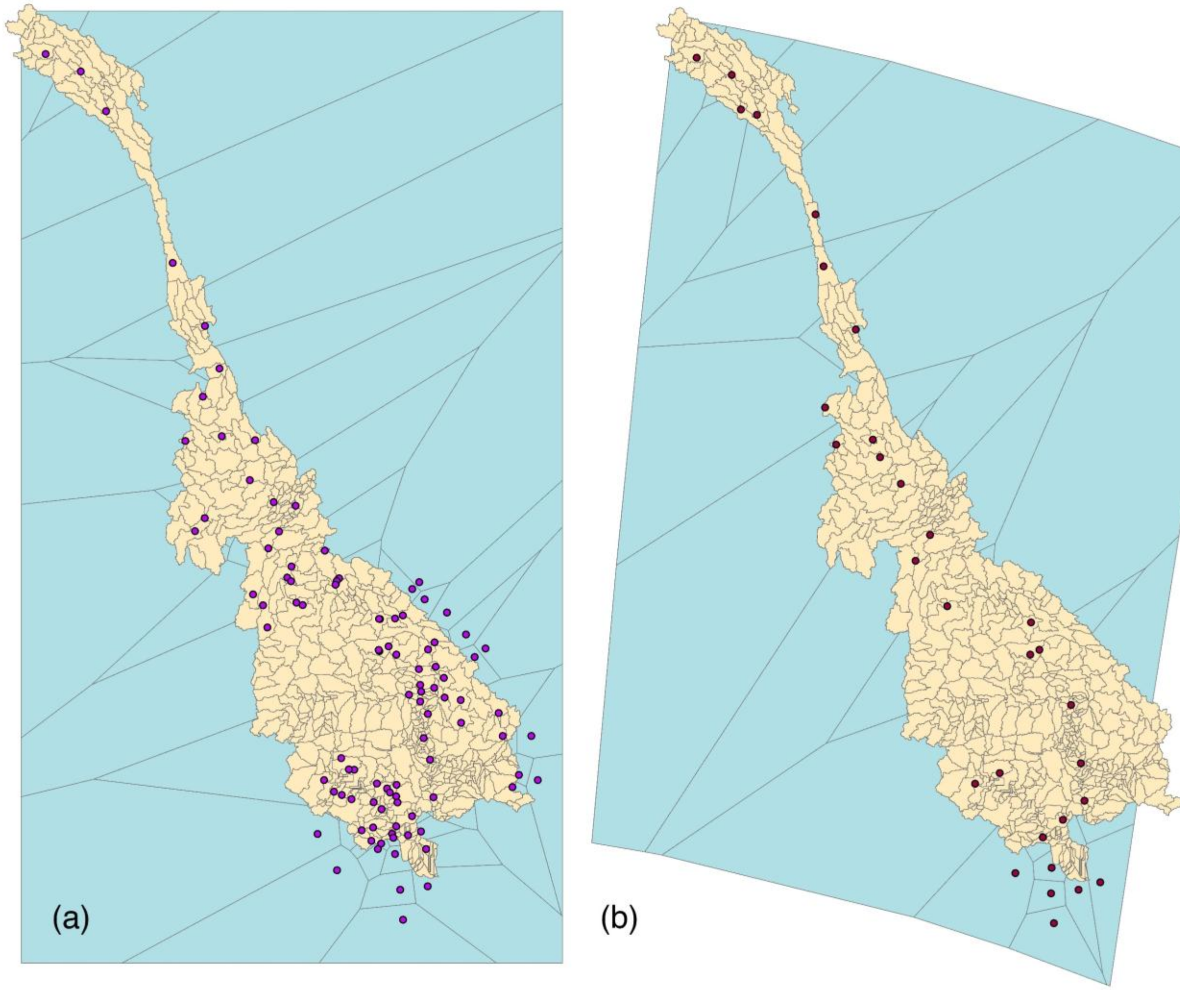

Figure S3. The location of stations for meteorological data, including (a) precipitation and (b) meteorological data including near-surface air pressure, air temperature, specific humidity, wind speed and direction, sunshine duration, and solar radiation.

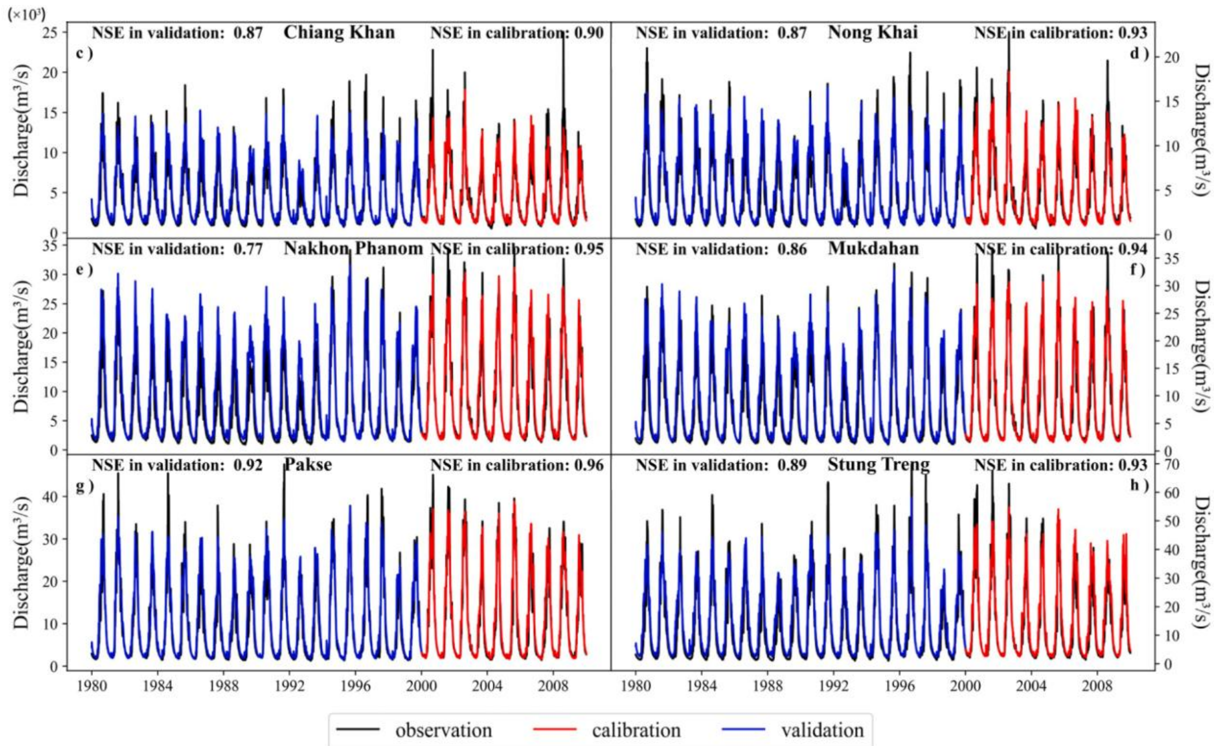

Figure S4. Comparison of time series discharge data produced by the THREW model and observed data at eight mainstream stations.

S3. Additional information for the developed hydrodynamic model

The performance of the hydrodynamic model was evaluated using time series of water level profiles, simulated discharge exchange between the Mekong mainstream and Tonle Sap Lake, and the accuracy of reverse flow period estimation.

Figure S5 presents a comparison of measured and simulated water level profiles from 2010 to 2020 at Prek Kdam and Kompong Luong stations. The hydrodynamic model successfully reproduces both high and low flow dynamics, with R^2 values exceeding 0.92 and RMSE values remaining within acceptable limits at both stations.

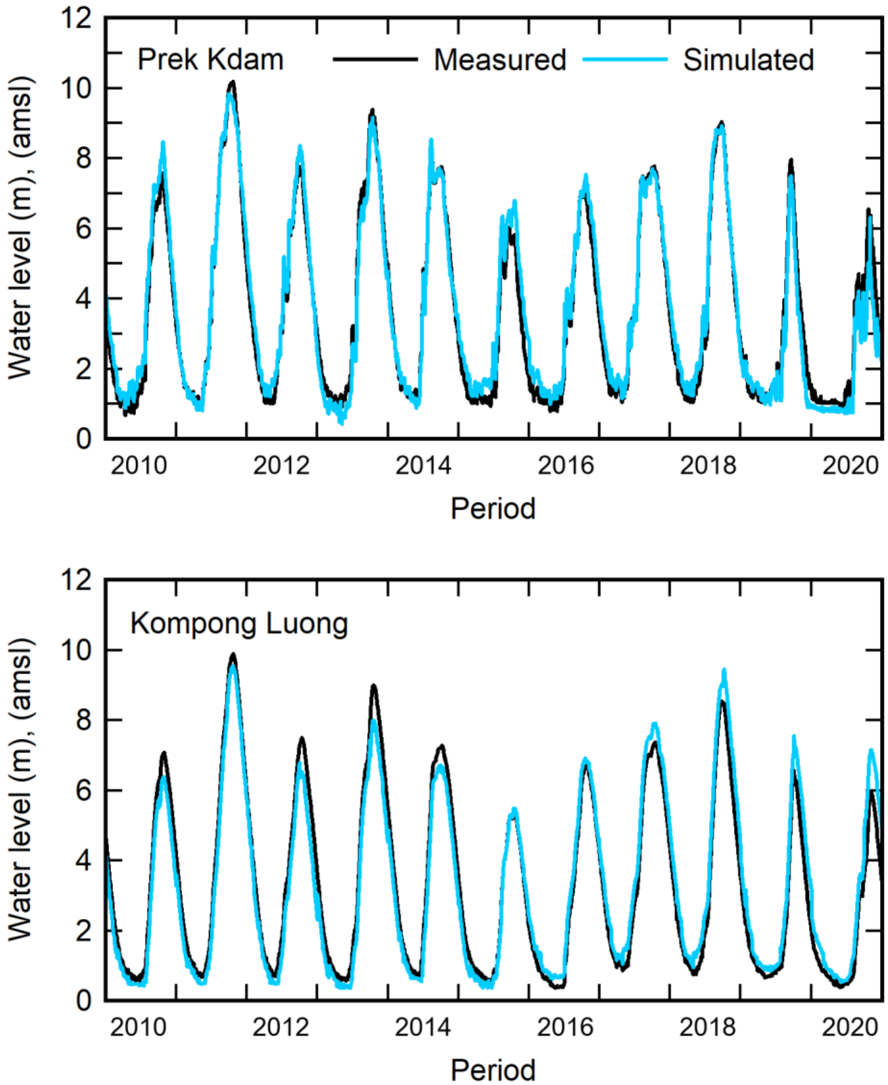

Figure S5. Comparison of measured and simulated water levels at Prek Kdam and Kompong Luong stations using the Delft3D-Flow model.

Figure S6 presents a comparison between measured and simulated exchanged discharge at Prek Kdam station during both reverse and non-reverse flow periods. All available measured discharge data are shown. A point-by-point comparison indicates that the model achieves high accuracy, with a mean relative error (MRE) of approximately 0.14, R^2 of ~0.94, and a Bias of $-89\ m^3\ s^{-1}$.

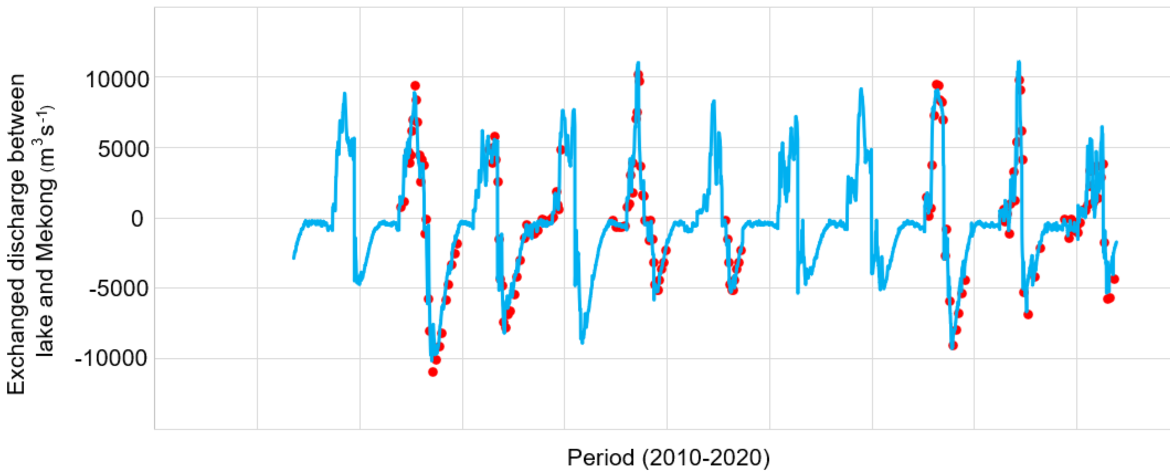

Figure S6. Comparison between measured and simulated exchanged discharge at Prek Kdam station. All available daily discharge data are shown. Positive values indicate inflow into Tonle Sap Lake, while negative values represent outflow from the lake to the Mekong River.

We also compared the simulated reverse flow periods with observed records from 2010 to 2024. The model accurately reproduced the timing of the reverse flow period, with discrepancies ranging from 0 to 3 days. This high level of accuracy indicates that the representation of canals, tributaries, and riverbed topography in the model is reasonably reliable.

Table S2. Comparison between simulated and observed reverse flow periods from 2010 to 2024 using the Delft3D-Flow model.

Year	Observed		Simulated		Differences
	Onset-End	Days	Onset-End	Days	
2010	July 10-October 23	106	July 11-October 26	107	+1
2011	May 30-September 29	123	May 29-September 26	121	-2
2012	May 27-September 21	118	May 30-September 23	116	-2
2013	Jun 17-October 4	109	Jun 16-October 6	112	+3
2014	Jun 15-September 7	84	Jun 15-September 6	84	0
2015	Jun 25-September 22	90	Jun 27-September 23	89	-1
2016	Jun 22-September 27	97	Jun 20-September 27	99	+2
2017	May 25-October 21	149	May 26-October 23	150	+1
2018	Jun 09- September 09	92	Jun 11- September 13	95	+3
2019	Jun 10- September 25	107	Jun 10- September 23	106	-1
2020	June 25-October 26	123	June 22-October 25	126	+3
2021	June 16-October 23	129	June 15-October 20	127	-2
2022	May 29-August 29	92	May 30-August 31	94	+2
2023	July 07-September 27	82	July 11-September 30	82	0
2024	June 28-October 01	95	June 27-October 01	96	+1